FMCW Radar Range Profile and Micro-Doppler Signature Fusion for Improved Traffic Signaling Motion Classification

Bidya Debnath, Iffat Ara Ebu, Sabyasachi Biswas,
Ali C. Gurbuz, and John E. Ball
Dept. of Electrical and Computer Engineering, Mississippi State University, MS, USA {bd1166, ie93, sb3682}@msstate.edu, {gurbuz, jeball}@ece.msstate.edu

Abstract—Human activity recognition plays a crucial role in Advanced Driver-Assisted Systems (ADAS). A significant challenge in achieving automotive autonomy lies in the difficulty faced by self-driving cars in navigating roads without operational traffic lights. In such scenarios, human intervention often involves directing vehicles through signaling with appropriate signs or gestures. This poses a considerable challenge for autonomous vehicles to interpret these gestures effectively. This study focuses on leveraging a dataset of traffic signaling motions obtained through millimeter-wave (mmWave) radar, a technology commonly used in the US traffic system. In this paper, we developed multimodal convolutional neural networks (CNN), considering both data fusion and feature fusion of radar range profiles and micro-doppler $(\mu$ -D) signatures, and compared the results with Unimodal CNNs on range profile and μ -D signatures. The findings indicate that the fusion-based CNNs outperform unimodal CNNs based on individual radar range profiles and μ -D signatures by about 10% and 6.5% respectively. Specifically, the accuracy achieved through multimodal CNNs reached around 92% and 96% for data-level and feature-level fusion respectively, showcasing the effectiveness of combining information from both modalities in enhancing human gesture recognition in trafficdirecting scenarios.

Index Terms—Range Profile, Micro-Doppler (μ -D), traffic gesture classification, CNN, Data fusion, ADAS, Feature fusion.

I. INTRODUCTION

N recent years, due to the popularity of radio-frequency (RF) sensors, sensing technologies have witnessed a remarkable transformation. The introduction of affordable solidstate transceivers and powerful graphics processing units (GPUs) has fueled the adoption of RF sensors across a wide range of applications. These sensors offer compelling advantages, including advanced sensing capabilities, compact size, and cost-effectiveness, making them an ideal choice for applications such as ADAS and autonomous systems. Simultaneously, deep learning (DL) has revolutionized various domains, including human activity recognition (HAR), by enabling the extraction of meaningful representations directly from data. This capability has significantly enhanced the performance of radar-based HAR systems, surpassing the benchmarks achieved in previous decades [1]. Radar has experienced a notable surge in popularity in recent decades across various applications. These applications encompass defense and security [2],the classification of Unmanned Aerial Vehicles

(UAVs) [3], ADAS [4], indoor monitoring human activity recognition [5]–[7], sign language recognition [8], and contactless health monitoring [9].

In Advanced Driver Assistance Systems (ADAS) and autonomous vehicle (AV) systems, radar serves as a fundamental sensing component [10], [11]. While AVs are currently trained to operate effectively under optimal road conditions, real-world scenarios often necessitate human guidance for safe and efficient navigation. These instances are particularly prevalent in dynamic traffic environments such as construction zones, school areas, or congested intersections, where automated traffic signals may be malfunctioning or unavailable. In such situations, traffic officers, school officials, or construction workers often provide directions to facilitate safe passage. To navigate these scenarios autonomously, AVs must be equipped with the capability to recognize and interpret human traffic guidance [12].

Research has been conducted to comprehend the efficacy of different sensor fusion, including mmWave automotive radar and lidar system [13], for the purpose of recognizing gestures made by human traffic directors. Combining data from both lidar and radar systems can potentially provide better results than relying on either technology individually, but by enhancing the classification algorithm associated with radar data, the system may achieve satisfactory results at a lower cost compared to incorporating lidar technology. [14].

While optical sensing [15], range profile [16], range doppler [17], [18] and μ -D [10] from radar signal have been investigated seperately in this domain, combining range profile and μ -D signature has not been previously examined for this specific problem. The study focuses on 12 distinct motions commonly employed in directing traffic within the U.S. traffic system. Initially, a dataset is gathered in a laboratory setting involving 14 participants. This dataset is acquired using mmWave radars and a motion-capture system, which captures the positions of the participants' body parts as they execute traffic directions. The dataset focuses on scenarios with individual human directors following pre-defined classes of directions within the line of sight of the sensor suite.

This paper concentrates specifically on the mmWave radar, demonstrating its effectiveness in comprehending human traf-

fic directions. Among various radar types, the Frequency Modulated Continuous Wave (FMCW) radar has emerged as the most extensively utilized for hand gesture recognition. This radar system emits an RF signal that undergoes a linear frequency sweep across its bandwidth, facilitating the capture of both range and velocity data. The FMCW radar records the Intermediate Frequency (IF) signal, storing the collected information in a three-dimensional structure termed a radar data cube (RDC) [19]. Several data representations can be extracted using FMCW radar, including μ -D spectrograms, range profile, and range-Doppler maps which can be used to train a machine learning (ML) model for gesture classification. These data representations or features extracted from them can be used to train a gesture classifier [20]. At first, timefrequency domain transformation [21] is done then range profile and μ -D signatures have been generated from the collected radar data cubes . Afterwards, the range profile data and μ -D signatures have been converted to images and classified using the developed convolutional neural network (CNN) architecture. The approach employed here is data-level fusion, a technique that manages raw data at the foundational level of the system with minimal loss and maximum reliability [22]. This method involves combining the resulting data and using it as input for both the training and classification processes in the model. Furthermore, the approach employs featurelevel fusion to enhance the correlation between corresponding features in two distinct datasets while emphasizing differences across various data points [23].

In the upcoming sections of this paper the analysis of the dataset will be presented. The paper is organized as follows: the experimental setup and dataset is provided in Section II, mmWave FMCW radar signal model, range profile, and microdoppler spectrogram generation are discussed in the Section III. The development of CNN architecture, unimodal and multimodal neural network are defined in section IV, and Section V presents the evaluation results of the proposed algorithm. Finally, Section VI concludes the paper and discusses future works.

II. EXPERIMENTAL SET UP & DATASET

A. Experimental set up

The dataset used for the purpose of this research was collected from the authors of paper [10], [13]. Data collection involved utilizing a Texas Instruments AWR2243 mmWave automotive FMCW radar. Before data collection, the radar was situated atop a table at an elevation of 1 meter. Participants were positioned 3 meters in front of the radar. A computer display, placed to the left of the radar but outside its field of view (FOV), presented prompts specifying the required gestures. Data collection spanned 155 seconds, during which four distinct gestures were performed, each repeated five times. A 1-second gap separated repetitions, and a 10-second interval followed each gesture for previewing the next one. Each sample had a duration of approximately 5 seconds.

Table I shows the parameters set for the AWR2243 radar for the experiment.

TABLE I: AWR2243 Radar Parameters [10]

Parameter	Value	
Starting Frequency	77 GHz	
Frequency Slope	66 MHz/μs	
Bandwidth	3960 MHz	
Pulse Repetition Interval (PRI)	161.29 μs	
Sampling Rate	18750 kHz	
ADC Samples No	256	
Number of TX Channels	3	
Number of RX Channels	4	
RX Gain	48 dB	
Periodicity	40 ms	
Number of Chirp Loops per Frame 248		
Number of Frames	3875	
Total Time	155 sec	

B. Dataset

The data collection experiment was conducted using 14 participants. The dataset comprises 840 samples, with each of the 12 distinct gestures represented by 70 samples. For this study, a dataset consisting 12 traffic signalling motions are based on US traffic system. These motions are designed to direct an oncoming vehicle to either stop, move from the stopping point in one of three directions, or to have traffic in any given position wait for other traffic to proceed onto the road. The gestures involve movement of not only the arms of the participants but also the hands, as well as the rotation of the head to look in specific directions.

Short description of each motion is given below.

- Stop extending the right arm straight in front with an open hand.
- 2) **Go** extending both hands straight, then flex both elbows towards the shoulders.
- 3) **Continue** extending the right arm forward with the elbow extended, then flex the right elbow towards the right shoulder.
- 4) **Left Turn** extending the right arm sideways and pointing right. Simultaneously, extend the left arm and flex the left elbow towards the left shoulder.
- 5) **Right Turn** extending the left arm sideways and pointing left. Simultaneously, extend the right arm and flex the right elbow towards the left shoulder.
- 6) **Stop Left, Go Front** Halt left traffic, then signal forward by extending the right arm sideways. Simultaneously, extend the left arm forward and flex the left elbow towards the right shoulder.
- 7) **Stop Right, Go Front** Halt left traffic, then signal forward by extending the right arm sideways. Simultaneously, extend the left arm forward and flex the left elbow towards the right shoulder.
- 8) **Stop Both Sides, Go Front** –Halt both sides, then signal forward by raising both shoulders and extending both
- 9) **Stop Front, Go Right** Halt, then signal right by extending the right hand forward with an open hand. Simultaneously, raise the left arm and flex the left elbow towards the shoulder.

- 10) **Stop Front, Go Left** Halt, then signal left by extending the left hand forward with an open hand. Simultaneously, raise the right arm and flex the right elbow towards the shoulder.
- 11) **Stop Front, Go Back** Halt, then signal backward by extending the left hand forward. Turn the torso right, raise the right arm, and flex the right elbow towards the right shoulder.
- 12) **Stop Back, Go Front** Halt back traffic, then signal forward by turning the torso right, raising the right arm, and extending the elbow.Move the left hand forward, flexing the left elbow towards the left shoulder.

III. DATA PROCESSING

A. Radar Signal Model

FMCW radar operation involves emitting continuous RF chirps, with key components including transmitters, receivers, mixers, and analog-to-digital converters (ADC) [24]. Reflected signals from objects are mixed with a local oscillator signal to produce an IF signal, then converted from analog to digital. Signal processing algorithms analyze the digital signal to calculate range and velocity. The frequency shift between transmitted and received signals determines distance, and the rate of change indicates velocity. Processed data is interpreted for insights into the target's location, speed, and other characteristics.

The chirp signal can be modeled as,

$$f_c(t) = f_s + \frac{BW}{\tau}t, t \subseteq [0, \tau]$$
 (1)

 $f_c(t)$ = The instantaneous frequency of the chirp signal in Hz. μ -D signals due to its inability to provide time-dependent frequency f_s = The initial frequency at time, t = 0s. quency information. To address this limitation, time-frequency

BW =The bandwidth in Hz.

 $\tau =$ The sweep time in seconds.

The FMCW radar records received samples in a structure known as the radar data cube (RDC). The RDC's rows correspond to fast-time samples or ADC values, while columns represent slow-time samples or the chirp loops transmitted by the radar. The third dimension of the RDC represents different RX channels.

The raw radar signal was of the size $N \times M \times R$, where, N denotes the number of fast-time samples, M is the number of pulses and R is no of receiver channels. We will only be working with data from one channel. So, the value of R is 1.

Various RF data representations, such as range-profile (RP) or μ -D signatures, can be generated through Fourier processing over the radar data cube (RDC).

B. Range Profile Generation

A range profile in radar is a representation of the radar return signal's strength as a function of distance from the radar antenna. It provides information about the distribution of echoes along the radial direction, aiding in target detection, localization, and identification [25].

The formula for the range profile P(n) is typically expressed as:

$$P(n) = |FFTs[n]| \tag{2}$$

Where, s[n] = Windowed received radar signal power. and

$$s[n] = (x * h)[n] = \sum_{-\infty}^{\infty} x[k] \cdot h[t - k]$$

x[n]=The received radar signal.

h[n] =Window of length 256 along fast time.

So, the range profile was calculated as in equation (3)

$$P(n) = \frac{\text{FFT}(s[n], N, dim)}{\sum h[n]}$$
 (3)

 $N = \text{Order of FFT} = 2^{10}$.

dim = Dimension along which the Fourier transform (FT) is taken, for our case, row-wise FT i.e., along the fast-time samples of each column.

 $\sum h[n]$ is used to scale down the received radar data after windowing.

C. Micro-doppler Spectrogram Generation

 μ -D in radar refers to frequency changes induced by small oscillating movements in a target, such as the spinning propellers of an aircraft or the constant movement of a human's arms and legs during walking [26]. These movements result in frequency modulations in the radar signal, providing valuable information about the kinematic properties of the target.

The Fourier Transform (FT) is not suitable for analyzing μ -D signals due to its inability to provide time-dependent frequency information. To address this limitation, time-frequency analysis techniques are employed, capturing both spectral and temporal information of μ -D signals. The μ -D information in radar signals is often visualized using a spectrogram, a widely used method that simultaneously depicts changes in both time and frequency domains. The μ -D spectrogram, typically generated using the Short-Time Fourier Transform (STFT) [27], allows for effective analysis of time-varying spectral content.

The μ -D spectrogram can be generated by using the STFT equations (4) and (5).

$$STFT[x[n]]_{m,\omega} = X[m,\omega] = \sum_{n=-\infty}^{\infty} x[n]w[n-m]e^{-j\omega n}$$
(4)

Spectrogram $[x[n]]_{m,\omega} = |X[m,\omega]|^2$ (5)

The STFT employs a Fourier Transform (FT) with a windowing function, as opposed to taking the FT of an entire signal in one step. Window size = 256×256 ;

Window shifting stride= 56; The spectrogram is derived from the power output of the STFT.

The radar transmits chirp signals towards the radar field of view. As the subject is in the radar field of view, some of the

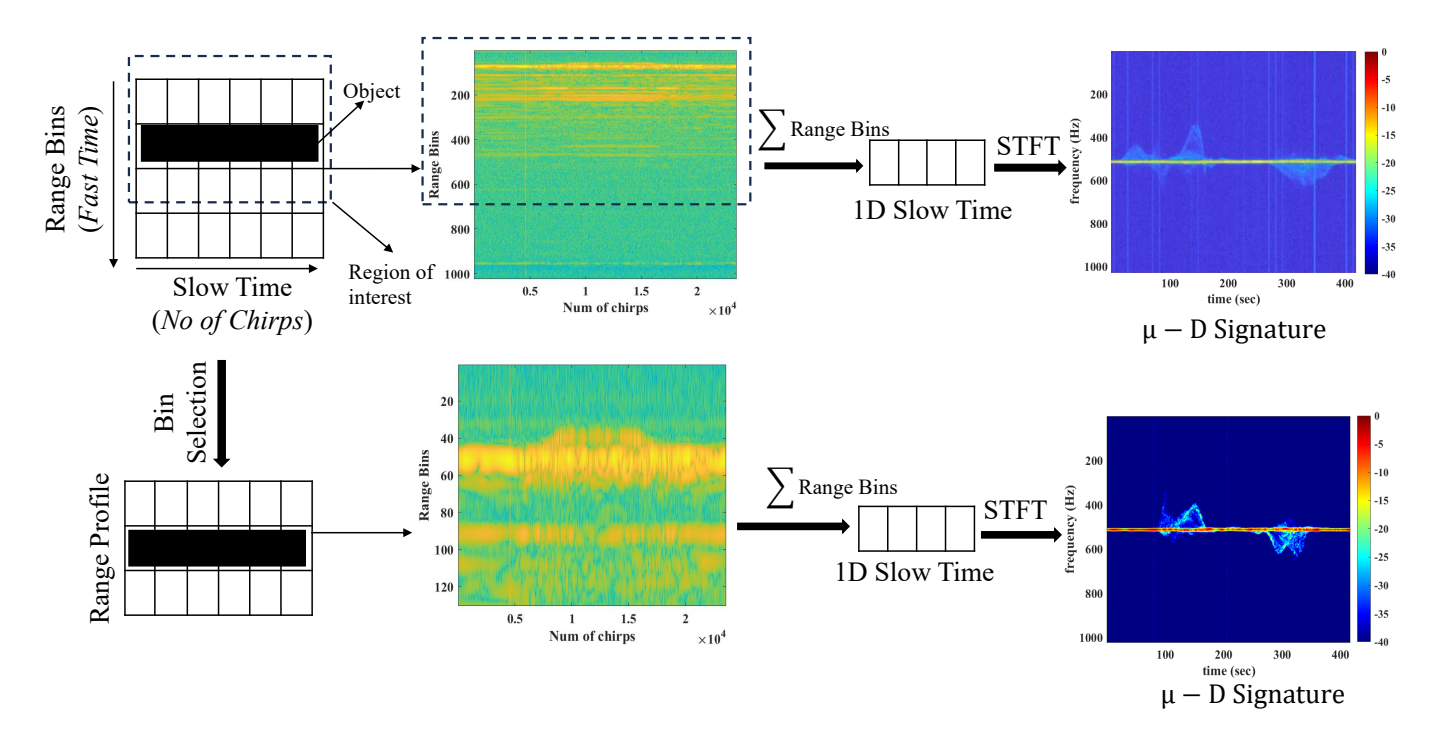


Fig. 1: Noise removal for μ -D generation from raw Radar data.

signal reflects from the subject and is received by the radar as a time-delayed, frequency-shifted version of the transmitted signal. Meanwhile, the transmitted signal travels beyond the subject and reflects from the wall behind, which is also picked up by the radar.

We can consider range bins closer to the subject as shown in Figure 1. This way we can mitigate insertion of noise as the large empty space behind the subject can contribute to noise signals.

We have converted both range profile and μ -D images to grayscale and resized them to 128×128 images for using them as input to CNN model.

IV. THE CNN ARCHITECTURE DEVELOPMENT

Two unimodal 2D CNN model had been developed for the classification of range profile and μ -D respectively. Two multimodal 2D CNN networks had been developed to implement data-level fusion and feature-level fusion of range profiles and μ -D images. The total number of epochs were taken to be 100 for each CNN model. Adam optimizer was used to train the epoch with a learning rate of 0.001.

A. Unimodal Neural Network

The same CNN-2D architecture was used for range profile and μ -D. The range profiles and μ -D spectrograms were saved as 128x128 grayscale images. The unimodal CNNs are configured to handle input shapes of 128x128x1 for grayscale images. The unimodal CNN consists of one feature extraction module and one classification module. As shown

is Fig. 2(a) , the feature extraction module comprises four convolutional layers, each having 3×3 kernels, a stride of 1×1 , and featuring 32, 32, 64, and 64 filters, respectively. After each convolutional layer, batch normalization, ReLU activation, and 2×2 max-pooling operations are applied. Subsequently, the tensor undergoes flattening, entering a dense layer with a size of 128, a dropout of 0.2, and an activation with ReLU in the classification module of Fig. 2(b). The architecture concludes with a softmax classifier.

B. Multimodal Neural Network

- 1) Data-level fusion: Data-level fusion was applied by concatenating both range profiles and μ -D images as two channels of the CNN-2D input as shown in Fig. 2(c). Consequently, the combined input dimensions for each sample in the CNN became $128 \times 128 \times 2$. The CNN-2D model employed for data-level fusion maintains the identical architecture used for unimodal classification with one feature extraction module and one classification module as described in section IV-A.
- 2) Feature-level fusion: The architecture for feature-level fusion takes range profile and μ -D signature as separate inputs for two separate feature extraction modules shown in Fig. 2(d). The output of the two feature extraction modules are concatenated. Subsequently, a dense layer with a size of 128, a ReLU activation layer, and a dropout layer with a rate of 0.2 was applied to the concatenate module output. The model concludes with a softmax classification layer.

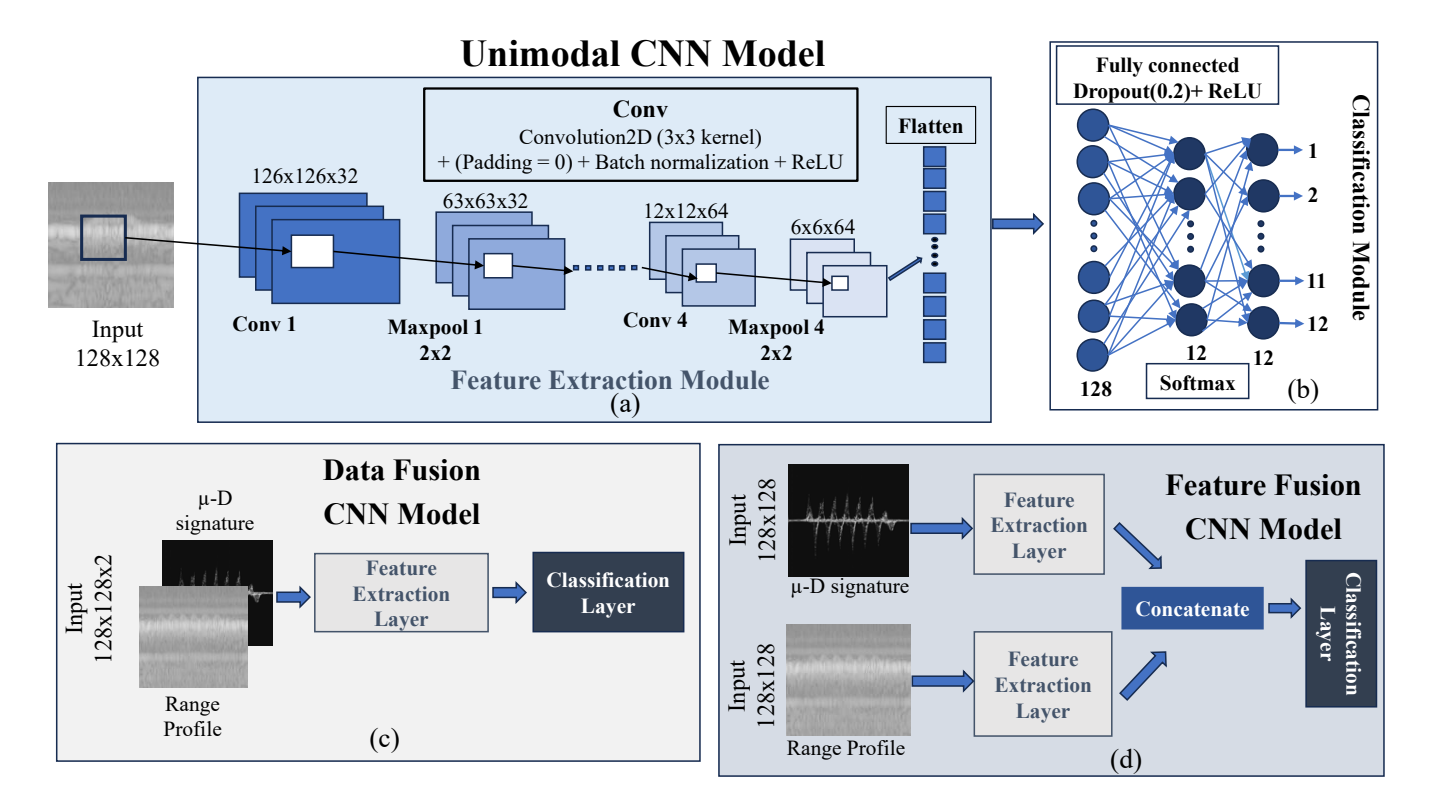


Fig. 2: Architectures for unimodal and multimodal CNN (a) feature extraction module, (b) classification module, (c)data fusion model, (d) feature fusion model

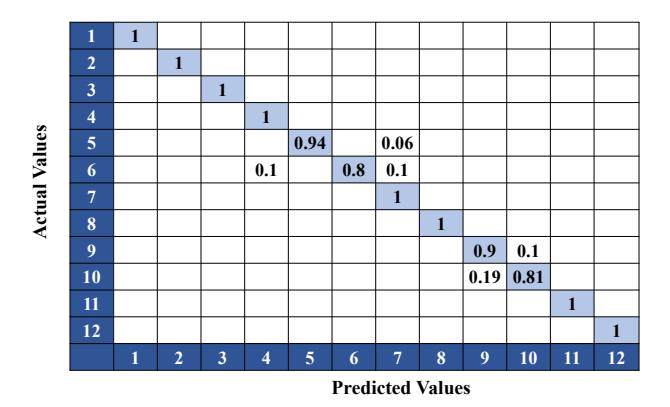


Fig. 3: Confusion matrix of Feature Fusion CNN (gray-scale) for 12 class traffic gestures' data.

V. PERFORMANCE ANALYSIS

Regarding classification, the dataset was partitioned into an 80% training set and a 20% testing set.

The outcomes are presented in Table II. Specifically focusing on grayscale images, the unimodal model achieves accuracy scores of 85.71%, 89.28% for range profile, μ -D respectively. For data fusion, and feature fusion models, 91.67%, and 95.83% accuracies are achieved respectively. Notably, feature fusion exhibits the highest accuracy among all CNN networks. Regarding precision, recall, and F1 score, the CNN for feature fusion demonstrates best performance with scores

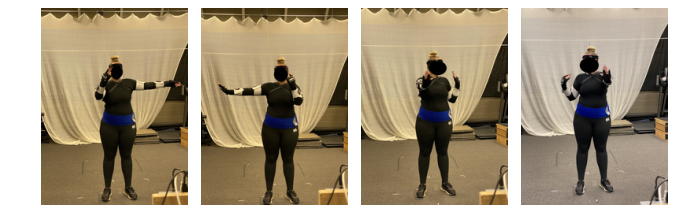


Fig. 4: The four traffic gestures that caused the network confusion

of 95.93%, 95.47%, and 95.48%, respectively. The confusion matrix in Fig. 3 illustrates the model's promising performance across most classes. For classes five, six, nine, and ten the network performs worse compared to other classes. The Fig 4 shows the instances of these gestures. In correspondence to the position of radar, these movements do not show much variation, as the movements are parallel to the radar surface. Specially, considering one channel of the radar, it is difficult to pick up lateral movements.

Despite the dataset's challenging nature due to movement variations among individuals, as discussed in [10], the proposed CNN model for feature fusion effectively addresses the dataset's complexities. This showcases significant potential and underscores its importance as a valuable feature for incorporation into ADAS systems.

TABLE II: Performance Comparison

Network	Testing Accuracy	Precision	Recall	F1 Score
Range Profile	85.71	85.51	85.15	87.74
Micro-doppler (μ-D)	89.28	89.10	89.49	88.60
Data Fusion	91.67	91.05	91.77	91.10
Feature Fusion	95.83	95.93	95.47	95.48

VI. CONCLUSION AND FUTURE WORK

The primary objective of this investigation is to conduct an initial exploration into the efficacy of data fusion and feature fusion techniques applied to range profile and μ -D data obtained from radar systems. The focus is on autonomously recognizing gestures from human traffic directors, facilitated by Convolutional Neural Networks (CNNs). The analysis of radar data reveals promising outcomes, demonstrating enhanced accuracy in classifying predefined traffic direction categories. Notably, these initial findings pertain to single traffic directions within a controlled laboratory setting.

Future works will encompass more realistic scenarios, incorporating multiple channels to improve classification accuracy for lateral movements with respect to subject body. Additionally, there is a plan to perform classification using range-Doppler data, The dataset used in this article also holds lidar and camera data. Lidar and camera data can be incorporated with radar data to improve classification accuracy as well.

VII. ACKNOWLEDGEMENTS

The data collection work was funded in part by the National Science Foundation (NSF) Awards #1931861, and #2047771. Human studies research was conducted under Mississippi State University Institutional Review Board (IRB) Protocol # IRB-21-256.

REFERENCES

- [1] S. Gurbuz, Ed., *Deep Neural Network Design for Radar Applications*. London: IET, 2020.
- [2] F. Fioranelli, M. Ritchie, and H. Griffiths, "Classification of unarmed/armed personnel using the netrad multistatic radar for microdoppler and singular value decomposition features," *IEEE Geoscience and Remote Sensing Letters*, vol. 12, no. 9, pp. 1933–1937, 2015.
- [3] A. Huizing, M. Heiligers, B. Dekker, J. de Wit, L. Cifola, and R. Harmanny, "Deep learning for classification of mini-uavs using micro-doppler spectrograms in cognitive radar," *IEEE Aerospace and Electronic Systems Magazine*, vol. 34, no. 11, pp. 46–56, 2019.
- [4] G. Hakobyan and B. Yang, "High-performance automotive radar: A review of signal processing algorithms and modulation schemes," *IEEE Signal Processing Magazine*, vol. 36, no. 5, pp. 32–44, 2019.
- [5] S. Z. Gurbuz and M. G. Amin, "Radar-based human-motion recognition with deep learning: Promising applications for indoor monitoring," *IEEE Signal Processing Magazine*, vol. 36, no. 4, pp. 16–28, 2019.
- [6] E. Kurtoğlu, S. Biswas, A. C. Gurbuz, and S. Z. Gurbuz, "Boosting multi-target recognition performance with multi-input multi-output radar-based angular subspace projection and multi-view deep neural network," *IET Radar, Sonar & Navigation*, vol. 17, no. 7, pp. 1115–1128, 2023.
- [7] A. Dahal, S. Biswas, and A. C. Gurbuz, "Comparison between wifi-csi and radar-based human activity recognition," in *Proc.* 2024 IEEE Radar Conference (RadarConf24), 2024.

- [8] S. Z. Gurbuz, A. C. Gurbuz, E. A. Malaia, D. J. Griffin, C. S. Crawford, M. M. Rahman, E. Kurtoglu, R. Aksu, T. Macks, and R. Mdrafi, "American sign language recognition using RF sensing," *IEEE Sensors Journal*, vol. 21, no. 3, pp. 3763–3775, 2021.
- [9] F. Fioranelli and J. L. Kernec, "Contactless radar sensing for health monitoring," in *Engineering and Technology for Healthcare*, 2021, pp. 29–59.
- [10] S. Biswas, B. Bartlett, J. E. Ball, and A. C. Gurbuz, "Classification of traffic signaling motion in automotive applications using fmcw radar," in 2023 IEEE Radar Conference (RadarConf23), 2023, pp. 1–6.
- [11] F. Islam, M. M. Nabi, and J. E. Ball, "Off-road detection analysis for autonomous ground vehicles: A review," *Sensors*, vol. 22, no. 21, 2022. [Online]. Available: https://www.mdpi.com/1424-8220/22/21/8463
- [12] N. Kern, L. Paulus, T. Grebner, V. Janoudi, and C. Waldschmidt, "Radar-based gesture recognition under ego-motion for automotive applications," *IEEE Transactions on Radar Systems*, vol. 1, pp. 542–552, 2023.
- [13] S. Biswas, J. E. Ball, and A. C. Gurbuz, "Radar-lidar fusion for classification of traffic signaling motion in automotive applications," in 2023 IEEE International Radar Conference (RADAR), 2023, pp. 1–5.
- [14] I. Bilik, "Comparative analysis of radar and lidar technologies for automotive applications," *IEEE Intelligent Transportation Systems Magazine*, vol. 15, no. 1, pp. 244–269, 2023.
- [15] C. Li and S. Yang, "Traffic police gesture recognition for autonomous driving," in 2018 IEEE 4th International Conference on Computer and Communications (ICCC), 2018, pp. 1413–1418.
- [16] S. Biswas and A. C. Gurbuz, "Deep learning based high-resolution frequency estimation for sparse radar range profiles," in *Proc. 2024 IEEE Radar Conference (RadarConf24)*, 2024.
- [17] Y. Sun, T. Fei, X. Li, A. Warnecke, E. Warsitz, and N. Pohl, "Real-time radar-based gesture detection and recognition built in an edge-computing platform," *IEEE Sensors Journal*, vol. 20, no. 18, pp. 10706–10716, 2020.
- [18] Y.-C. Jhaung, Y.-M. Lin, C. Zha, J.-S. Leu, and M. Köppen, "Implementing a hand gesture recognition system based on rangedoppler map," *Sensors*, vol. 22, no. 11, 2022. [Online]. Available: https://www.mdpi.com/1424-8220/22/11/4260
- [19] S. Biswas, C. O. Ayna, S. Z. Gurbuz, and A. C. Gurbuz, "Cv-sincnet: Learning complex sinc filters from raw radar data for computationally efficient human motion recognition," *IEEE Transactions on Radar Systems*, vol. 1, pp. 493–504, 2023.
- [20] S. Abouzaid, L. Nothelle, T. Jaeschke, and N. Pohl, "Fine hand gesture recognition using d-band fmcw radar," in 2023 20th European Radar Conference (EuRAD), 2023, pp. 246–249.
- [21] S. Biswas, C. O. Ayna, S. Z. Gurbuz, and A. C. Gurbuz, "Complex sincent for more interpretable radar based activity recognition," in 2023 IEEE Radar Conference (RadarConf23), 2023, pp. 1–6.
- [22] H. Zhou, Y. Zhao, Y. Liu, S. Lu, X. An, and Q. Liu, "Multi-sensor data fusion and cnn-lstm model for human activity recognition system," *Sensors*, vol. 23, no. 10, 2023. [Online]. Available: https://www.mdpi.com/1424-8220/23/10/4750
- [23] S. He, Y. Wang, X. Du, Z. Gui, X. Ren, and X. Yin, "icar: Multi-modal learning-inspired vehicle owner recognition based on fmcw radar in internet of things," in 2023 IEEE/CIC International Conference on Communications in China (ICCC), 2023, pp. 1–6.
- [24] J. J. Lin, Y. P. Li, W. C. Hsu, and T. S. Lee, "Design of an fmcw radar baseband signal processing system for automotive application," *SpringerPlus*, vol. 5, pp. 1–16, 12 2016. [Online]. Available: https://springerplus.springeropen.com/articles/10.1186/s40064-015-1583-5
- [25] J. Portegies Zwart and E. Beheer, "Aircraft recognition from features extracted from measured and simulated radar range profiles," Amst.: Eigen Beheer, 2003.
- [26] T. Thayaparan, S. Abrol, and E. S. Riseborough, Micro-Doppler radar signatures for intelligent target recognition. Defence R & D Canada-Ottawa, 2004.
- [27] A. Hanif, M. Muaz, A. Hasan, and M. Adeel, "Micro-doppler based target recognition with radars: A review," *IEEE Sensors Journal*, vol. 22, no. 4, pp. 2948–2961, 2022.